

Effect of astrocyte on synchronization of thermosensitive neuron-astrocyte minimum system

Yi-Xuan Shan(单仪萱), Hui-Lan Yang(杨惠兰), Hong-Bin Wang(王宏斌), Shuai Zhang(张帅), Ying Li(李颖), and Gui-Zhi Xu(徐桂芝)

Citation: Chin. Phys. B, 2022, 31 (**8**): 080507. DOI: 10.1088/1674-1056/ac490c
Journal homepage: http://cpb.iphy.ac.cn; http://iopscience.iop.org/cpb

What follows is a list of articles you may be interested in

Power-law statistics of synchronous transition in inhibitory neuronal networks

Lei Tao(陶蕾) and Sheng-Jun Wang(王圣军)
Chin. Phys. B, 2022, 31 (**8**): 080505. DOI: 10.1088/1674-1056/ac5c31

Explosive synchronization: From synthetic to real-world networks

Atiyeh Bayani, Sajad Jafari, and Hamed Azarnoush
Chin. Phys. B, 2022, 31 (**2**): 020504. DOI: 10.1088/1674-1056/ac3cb0

Explosive synchronization in a mobile network in the presence of a positive feedback mechanism

Dong-Jie Qian(钱冬杰)
Chin. Phys. B, 2022, 31 (**1**): 010503. DOI: 10.1088/1674-1056/ac16d3

Dynamic modeling and aperiodically intermittent strategy for adaptive finite-time synchronization control of the multi-weighted complex transportation networks with multiple delays

Ning Li(李宁), Haiyi Sun(孙海义), Xin Jing(靖新), and Zhongtang Chen(陈仲堂)
Chin. Phys. B, 2021, 30 (**9**): 090507. DOI: 10.1088/1674-1056/abea92

Dynamical response of a neuron-astrocyte coupling system under electromagnetic induction and external stimulation

Zhi-Xuan Yuan(袁治轩), Pei-Hua Feng(冯沛华), Meng-Meng Du(独盟盟), Ying Wu(吴莹)
Chin. Phys. B, 2020, 29 (**3**): 030504. DOI: 10.1088/1674-1056/ab7441

Effect of astrocyte on synchronization of thermosensitive neuron–astrocyte minimum system

Yi-Xuan Shan(单仪萱)[1,2], Hui-Lan Yang(杨惠兰)[1,2], Hong-Bin Wang(王宏斌)[1,2,†], Shuai Zhang(张帅)[1,2], Ying Li(李颖)[1,2], and Gui-Zhi Xu(徐桂芝)[1,2]

[1] *State Key Laboratory of Reliability and Intelligence of Electrical Equipment, Hebei University of Technology, Tianjin* 300130, *China*
[2] *Hebei Key Laboratory of Bioelectromagnetics and Neural Engineering, Hebei University of Technology, Tianjin* 300130, *China*

(Received 13 October 2021; revised manuscript received 30 December 2021; accepted manuscript online 7 January 2022)

Astrocytes have a regulatory function on the central nervous system (CNS), especially in the temperature-sensitive hippocampal region. In order to explore the thermosensitive dynamic mechanism of astrocytes in the CNS, we establish a neuron–astrocyte minimum system to analyze the synchronization change characteristics based on the Hodgkin–Huxley model, in which a pyramidal cell and an interneuron are connected by an astrocyte. The temperature range is set as 0 °C–40 °C to juggle between theoretical calculation and the reality of a brain environment. It is shown that the synchronization of thermosensitive neurons exhibits nonlinear behavior with changes in astrocyte parameters. At a temperature range of 0 °C–18 °C, the effects of the astrocyte can provide a tremendous influence on neurons in synchronization. We find the existence of a value for inositol triphosphate (IP_3) production rate and feedback intensities of astrocytes to neurons, which can ensure the weak synchronization of two neurons. In addition, it is revealed that the regulation of astrocytes to pyramidal cells is more sensitive than that to interneurons. Finally, it is shown that the synchronization and phase transition of neurons depend on the change in Ca^{2+} concentration at the temperature of weak synchronization. The results in this paper provide some enlightenment on the mechanism of cognitive dysfunction and neurological disorders with astrocytes.

Keywords: astrocytes, synchronization, Hodgkin–Huxley model, thermosensitive neuron

PACS: 05.45.–a, 64.70.qj, 87.19.L–, 87.19.lk **DOI:** 10.1088/1674-1056/ac490c

1. Introduction

The brain contains copious and complex dynamic characteristics, and is the most significant information processing system. Synchronization of neuronal discharge activities is a typical dynamics phenomenon in complex systems, and plays an especially vital role in the brain function of information processing.[1,2] The complex network of the central nervous system (CNS) plays a critical role in the maintenance of many activities including cognition and memory, in which the hippocampus is a typical region including pyramidal cells (excitatory neurons), interneurons (inhibitory neurons) and astrocytes.[3] From the perspective of complex networks, the resting state of the brain is the stable equilibrium points of the system, and the firing activity of neurons with external stimulation is the limit cycles of the system.[2] By means of external stimulation, the interference of chaotic synchronization and regulation of the phase coordination between systems can improve cognitive function and treat nervous system diseases.[4–6] Obviously, the global dynamic behavior of the system is very complex,[7–11] and is subject to many factors, such as network scale,[12,13] initial value sensitivity,[14,15] and system noise.[16–19] Therefore, it is very difficult to regulate the complex network. Based on the medical significance and theoretical value of neural regulation, the study of nonlinear dynamic characteristics of neuronal discharge has attracted increasing attention recently.

In the past decade, it has been reported that astrocytes are the main cells in the hippocampus, which interact with pyramidal cells and interneurons to provide structural, trophic and metabolic support.[20] Due to the loss of a Na^{2+} channel, astrocytes fail to generate action potential. Instead, astrocytes respond to neuronal activity by increasing the level of Ca^{2+} in neurons.[21,22] When firing, neurons produce neurotransmitters, such as glutamate and adenosine triphosphate (ATP), which bind to the transmitter receptors on astrocytes.[23] In this process, the production of inositol triphosphate (IP_3) is promoted with the release of Ca^{2+} by activating astrocytes.[24] With the increase in intracellular Ca^{2+} concentration, the astrocytes release glutamate, ATP and other glial transmitters back to the neurons.[24] These transmitters can regulate the information transmission and excitability of synapses.[25,26] In particular, Ca^{2+} oscillation plays a central role in neurons with a close relationship of periodic bursting oscillation.[27] According to the bidirectional feedbacks of astrocytes and neurons, a tripartite synapse is conceptualized.[20] It is indicated that the connection between presynaptic and postsynaptic neurons is regulated by astrocytes.[28]

Astrocytes can dynamically regulate neuronal excitability and synaptic plasticity. It is reported that astrocytes with the best coupling strength significantly improve the weak signal detection performance of neurons.[29] In addition, as-

†Corresponding author. E-mail: wanghongbin@hebut.edu.cn
© 2022 Chinese Physical Society and IOP Publishing Ltd

trocytes are confirmed to have significant consequences for synchronization. For example, it is found that healthy astrocytes may cause two neurons to lose synchronization.[22] Hence, astrocytes display an obvious function of regulating synapses, which can trigger neuronal desynchronization to a certain extent. Moreover, a recent study indicated that overactive astrocytes can produce a large amount of Ca^{2+}, leading to high-frequency discharge of neurons.[29] In this context, Øyehaug[30] revealed that the local uptake of astrocytes is an important factor in inducing epileptic discharge. In particular, it is observed that glial networks exhibit strong synchronization with high activity over long distances before epileptic seizures, rather than neurons with a small amount of synchronous activity locally.[31] Considering the above results of astrocytes, we establish a neuron–astrocyte minimum model to study the characteristics of neuronal discharge in this paper.

On the other hand, temperature (T) is a non-negligible factor in the nervous system. It has been shown that an increase in temperature increases the intrinsic excitability of excitatory pyramidal cells and inhibitory interneurons in the hippocampus.[32] With increasing temperature, the nervous system changes from a conventional spike discharge state to a chaotic burst state, and finally stabilizes to a conventional burst state.[33] Hence, it is obvious that the pyramidal cells and interneurons in the hippocampus are thermosensitive. At low temperature, with an increase in temperature, the neuronal clusters show the transition of desynchronization and burst synchronization, as well as promoting an in-phase synchronous state.[34] At high temperature, the low variability of burst intervals of neurons results in synchronization of phase. If it further increases, an over level temperature leads to spike synchronization.[35] In addition, temperature affects the action potential of neurons by regulating the conductance and gating kinetics of ion channels.[36–38] The experimental results show that alterations to the gating kinetics of ion channels are associated with temperature, which leads to changes in the inherent membrane excitability.[39] It has been experimentally verified that the input resistance of pyramidal cells and interneurons decreases with an increase in temperature.[32] Based on neural computing, temperature can affect the conductance of ion channels. Moreover, ion channel current can regulate the excitability of neurons.[36] Therefore, we establish a thermosensitive coupling model of pyramidal cells and interneurons for dynamics analysis.

Temperature not only affects the function of neurons, but can also cause changes in the activation intensity for astrocytes.[40] Experiments have shown that astrocytes have a slow increase in transient Ca^{2+} at warming temperature.[41] In addition, the metabolic cycle and activation degree of astrocytes are inhibited by lowering the temperature.[40] Hence, temperature variation can influence neural activities in brain, especially in the CNS with many astrocytes. Recently it was revealed that the ion channels associated with calcium are temperature sensitive in astrocytes, e.g., the TRP channel[42] and Kir.4.1 channel.[43] In addition, Zhang[42] showed that the calcium flow through IP_3 receptor channels in astrocytes is strongly dependent on temperature. Therefore, the IP_3 receptor channel is affected by temperature.

In this paper, we establish a thermosensitive neuron–astrocyte minimum system based on the Hodgkin–Huxley model. We focus on the inference of astrocyte parameters and temperature in the synchronization behavior by using the maximum synchronization error and phase difference. The results indicate that the production rate of IP_3 and feedback intensities of astrocytes induce the periodic oscillatory activity of IP_3 and Ca^{2+} concentration envelope curves. The synchronous phenomenon and asynchronous state between firing neurons at the temperature of weak synchronization is also explained.

The paper is organized as follows. In Section 2, we describe the details of the neuron–astrocyte minimum system based on the Hodgkin–Huxley neuron model with major parameters, which is indispensable in neuron dynamics and synchronization quantifications. In Section 3, we analyze the effects of positive and negative feedback intensities of astrocytes on neuronal synchronization, and the production rate of IP_3 on neuronal synchronization. We study the relationship between concentration of Ca^{2+} and synchronization further. Finally, the discussion and conclusion are presented in Section 4.

2. Model and methods

Based on the hippocampal CA1 neuron–astrocyte network structure, we establish the neuron–astrocyte minimum system shown in Fig. 1, which consists of a pyramidal cell, an interneuron and an astrocyte.[20] With regard to computation, we select a modified version of the Hodgkin–Huxley model[44] and Li–Rinzel calcium model[25] to apply to the minimum model. Moreover, it is reported that excitatory pyramidal cells and inhibitory interneurons in the hippocampus are sensitive to temperature.[32,45,46] Additionally, Stephan's experiment verified that astrocytes are temperature dependent.[41] Thus, we introduce a temperature factor into the minimum model reference to Ref. [47]. Based on the thermosensitive neuron–astrocyte minimum model, we study the synchronous regulation mechanism for the connection of pyramidal cells and interneurons through astrocytes.[48] The mathematical description of the improved neuron model is illustrated below.

The dynamics of the pyramidal cell are as follows:

$$C_{\mathrm{m}}\frac{\mathrm{d}V_{\mathrm{PY}}}{\mathrm{d}t} = -I_{\mathrm{Na}} - I_{\mathrm{K}} - I_{\mathrm{L}} + I_{\mathrm{ext}}^{\mathrm{PY}} + I_{\mathrm{syn}}^{\mathrm{PY}} + I_{\mathrm{astro}}^{\mathrm{PY}}. \tag{1}$$

The dynamics of the interneuron are as follows:

$$C_{\mathrm{m}}\frac{\mathrm{d}V_{\mathrm{IN}}}{\mathrm{d}t} = -I_{\mathrm{Na}} - I_{\mathrm{K}} - I_{\mathrm{L}} + I_{\mathrm{ext}}^{\mathrm{IN}} + I_{\mathrm{syn}}^{\mathrm{IN}} + I_{\mathrm{astro}}^{\mathrm{IN}}. \tag{2}$$

Here $C_{\rm m}$ represents the capacitance of the lipid bilayer, with a value of 1 μF/cm^2, and $I_{\rm ext}^{\rm PY}$ and $I_{\rm ext}^{\rm IN}$ are the external stimulation currents of the pyramidal cell and interneuron, respectively. They provide different stimulus intensities to the system. $V_{\rm PY}$ is the membrane potential of the pyramidal cell, and $V_{\rm IN}$ is the membrane potential of the interneuron. $I_{\rm astro}^{\rm PY}$ and $I_{\rm astro}^{\rm IN}$ denote the feedback currents produced by the astrocyte in response to neuronal spiking. In practice, the electrical activity of the neuron also depends upon the temperature environment to which the neuron is exposed. Thus, it is necessary to incorporate temperature into the neuron equation and cable model, which is inextricably linked with the neuron dynamics of the thermosensitive neuron–astrocyte minimum system.[39,49] The channel currents are given by the following balance equations:

$$\begin{aligned} &I_{\rm Na} = \rho g_{\rm Na} m^3 h (V_x - E_{\rm Na}), \\ &I_{\rm K} = \rho g_{\rm K} n^4 (V_x - E_{\rm K}), \\ &I_{\rm L} = g_{\rm L} (V_x - E_{\rm L}), \quad x = {\rm PY},\ {\rm IN}. \end{aligned} \tag{3}$$

where $g_{\rm Na} = 120\ {\rm ms}\cdot{\rm cm}^{-2}$, $g_{\rm K} = 36\ {\rm ms}\cdot{\rm cm}^{-2}$ and $g_{\rm L} = 0.3\ {\rm ms}\cdot{\rm cm}^{-2}$ are the maximum conductance of the sodium channel, potassium channel and leakage channel, respectively, $E_{\rm Na} = 50$ mV, $E_{\rm K} = -77$ mV, and $E_{\rm L} = -54.5$ mV are recorded as the sodium ion balance voltage, potassium ion balance voltage and leakage balance voltage, respectively. In addition, it is verified that temperature can affect the ion conductance and ion gate channel variable in neurons.[36,45–47] According to Ref. [47], the parameter ρ denotes the temperature scale factor of ion conductance in Eq. (3), for which the expression is shown below:

$$\rho = 1.3{\rm e}^{\frac{T-T_0}{10}}. \tag{4}$$

Moreover, in Eq. (3), the expression for sodium channels contains activation variable m and inactivation variable h, and that for potassium channels contain activation variable n. These activation variables and inactivation variables vary with the change in membrane potentials. The dynamics of the gating channel depend on the following equations:

$$\begin{aligned} &\frac{{\rm d}m}{{\rm d}t} = \psi(\alpha_m(1-m) - \beta_m m), \\ &\frac{{\rm d}h}{{\rm d}t} = \psi(\alpha_h(1-h) - \beta_h h), \\ &\frac{{\rm d}n}{{\rm d}t} = \psi(\alpha_n(1-n) - \beta_n n). \end{aligned} \tag{5}$$

Similarly, the parameter ψ denotes the temperature scale factor of the ion gating channel variable in Eq. (5), for which the expression is shown below:[47]

$$\psi = 3{\rm e}^{\frac{T-T_0}{10}}. \tag{6}$$

According to the results of experiments, T_0 is selected at 25 °C in Eqs. (4) and (6).[47] Specifically, the expressions of activation variables and inactivation variables in Eq. (5) are shown as follows:

$$\begin{aligned} &\alpha_m = \frac{0.1\,(V_x+40)}{1-{\rm e}^{\frac{-(V_x+40)}{10}}}, \\ &\beta_m = 4{\rm e}^{\frac{-(V_x+65)}{18}}, \\ &\alpha_h = 0.07{\rm e}^{\frac{-(V_x+65)}{20}}, \\ &\beta_h = \frac{1}{\left(1+{\rm e}^{\frac{-(V_x+35)}{10}}\right)}, \\ &\alpha_n = \frac{0.01\,(V_x+55)}{\left(1-{\rm e}^{\frac{-(V_x+55)}{10}}\right)}, \\ &\beta_n = 0.125{\rm e}^{\frac{-(V_x+65)}{80}}, \quad x = {\rm PY},\ {\rm IN}. \end{aligned} \tag{7}$$

The synaptic currents of $I_{\rm syn}^{\rm PY}$ and $I_{\rm syn}^{\rm IN}$ are expressed as follows:[35,50]

$$\begin{aligned} &[A]_x = \frac{1}{1+{\rm e}^{-\frac{V_x-\theta}{\delta}}}, \\ &\frac{{\rm d}s_x}{{\rm d}t} = \alpha_s [A]_x (1-s_x) - \beta_s s_x, \quad x = {\rm PY},\ {\rm IN}, \\ &I_{\rm syn}^{\rm PY} = g_{\rm si} s_{\rm IN} (V_{\rm si} - V_{\rm PY}), \\ &I_{\rm syn}^{\rm IN} = g_{\rm se} s_{\rm PY} (V_{\rm se} - V_{\rm IN}), \end{aligned} \tag{8}$$

where $g_{\rm si}$ and $g_{\rm se}$ are the inhibitory and excitatory coupling intensities, and $V_{\rm si}$ and $V_{\rm se}$ are the inhibitory and excitatory synaptic reversible potentials, respectively. $[A]_{\rm PY}$ and $[A]_{\rm IN}$ are the respective concentrations of neurotransmitters released by the pyramidal cell and interneuron, depending on their respective membrane potentials. The synaptic variables $s_{\rm PY}$ and $s_{\rm IN}$ reflect the effect of neurotransmitters that activate the neuron to release.

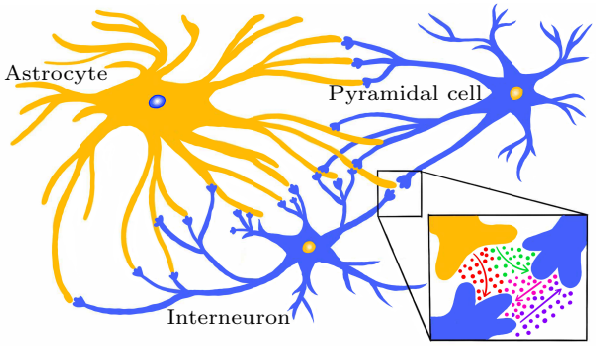


Fig. 1. Illustration of the neuron–astrocyte minimum system. The model includes a pyramidal cell (PY), interneuron (IN) and astrocyte (AS). The purple arrow represents the inhibitory coupling and the pink arrow represents the excitatory coupling between the pyramidal cell and interneuron. After the neurons have stimulated the astrocyte, the astrocyte feeds back to the pyramidal cell and the interneuron as currents, in which the red arrow represents the positive feedback to the inhibitory interneuron and the green arrow represents the negative feedback to the excitatory pyramidal cell.

When activated, the neuron releases a certain amount of neurotransmitters into the synaptic gap. The main neurotransmitters bind to the postsynaptic membrane. Other neurotransmitters can bind to astrocytes, resulting in the release of IP_3. The regulation of IP_3 in astrocytes can be expressed by the equation below:

$$\frac{\mathrm{d}[\mathrm{IP_3}]}{\mathrm{d}t} = \frac{1}{\tau_{\mathrm{IP_3}}}([\mathrm{IP_3}]^* - [\mathrm{IP_3}]) + r_{\mathrm{IP_3}}([A]_{\mathrm{PY}} + [A]_{\mathrm{IN}}), \quad (9)$$

where $[\mathrm{IP_3}]^*$ is the equilibrium concentration of IP_3, $\tau_{\mathrm{IP_3}}$ is the decay rate of IP_3, and $r_{\mathrm{IP_3}}$ is the production rate of IP_3. IP_3 promotes the release of Ca^{2+}. The kinetic equation of Ca^{2+} concentration is as follows:

$$\frac{\mathrm{d}[\mathrm{Ca^{2+}}]}{\mathrm{d}t} = -J_{\mathrm{channel}} - J_{\mathrm{pump}} - J_{\mathrm{leak}}, \quad (10)$$

where J_{channel} represents the calcium flux moving from the endoplasmic reticulum to the inner space of the astrocytes through the IP_3 channel, J_{pump} represents the pump flux pumped into the endoplasmic reticulum from the astrocytes, and J_{leak} is defined as the leakage flux from the endoplasmic reticulum to the astrocytes. The specific expressions are as follows:

$$\begin{aligned}
J_{\mathrm{channel}} &= \rho c_1 v_1 m_\infty^3 n_\infty^3 q^3([\mathrm{Ca^{2+}}] - [\mathrm{Ca^{2+}}]_{\mathrm{ER}}),\\
J_{\mathrm{pump}} &= \frac{v_3[\mathrm{Ca^{2+}}]^2}{k_3^2 + [\mathrm{Ca^{2+}}]^2},\\
J_{\mathrm{leak}} &= c_1 v_2([\mathrm{Ca^{2+}}] - [\mathrm{Ca^{2+}}]_{\mathrm{ER}}),\\
\frac{\mathrm{d}q}{\mathrm{d}t} &= \psi(\alpha_q(1-q) - \beta_q q),
\end{aligned} \quad (11)$$

where q is the activation variable of the IP_3 receptor on the endoplasmic reticulum surface, also affected by temperature.[42] The expressions of the parameters in Eq. (11) is as follows:

$$\begin{aligned}
m_\infty &= \frac{[\mathrm{IP_3}]}{[\mathrm{IP_3}] + d_1},\\
n_\infty &= \frac{[\mathrm{Ca^{2+}}]}{[\mathrm{Ca^{2+}}] + d_5},\\
[\mathrm{Ca^{2+}}]_{\mathrm{ER}} &= \frac{c_0 - [\mathrm{Ca^{2+}}]}{c_1},\\
\alpha_q &= a_2 d_2 \frac{[\mathrm{IP_3}] + d_1}{[\mathrm{IP_3}] + d_5},\\
\beta_q &= a_2[\mathrm{Ca^{2+}}].
\end{aligned} \quad (12)$$

According to Ref. [51], the feedback currents of astrocytes to neurons are described as follows:

$$\begin{aligned}
\frac{\mathrm{d}F}{\mathrm{d}t} &= -\frac{F}{\tau_{\mathrm{Ca^{2+}}}} + (1-F)k\Theta([\mathrm{Ca^{2+}}] - [\mathrm{Ca^{2+}}]_{\mathrm{th}}),\\
I_{\mathrm{astro}}^{\mathrm{PY}} &= -\varepsilon_1 F,\\
I_{\mathrm{astro}}^{\mathrm{IN}} &= \varepsilon_2 F,
\end{aligned} \quad (13)$$

where $\Theta(x)$ is the Heaviside ladder function, k is the scale factor, and $\tau_{\mathrm{Ca^{2+}}}$ is the relaxation time constant. When the calcium concentration of astrocytes exceeds $[\mathrm{Ca^{2+}}]_{\mathrm{th}}$, the feedback current of astrocytes to neurons can be activated. ε_1 and ε_2 represent the proportional coefficients of feedback currents of astrocytes, which are used to simulate the regulation of synaptic plasticity of neurons under the influence of astrocytes. When $\varepsilon_1 = \varepsilon_2 = 0$, astrocytes do not play a role in the synaptic plasticity of neurons.

According to Refs. [51,52], all necessary parameters in this paper are listed in Table 1.

Table 1. Parameters of the neuron–astrocyte minimum system.

Parameter	Value	Unit	Parameter	Value	Unit
C_{m}	1.0	$\mu\mathrm{F\cdot cm^{-2}}$	k_3	0.1	$\mu\mathrm{mol\cdot L^{-1}}$
g_{L}	0.3	$\mathrm{ms\cdot cm^{-2}}$	d_1	0.13	$\mu\mathrm{mol\cdot L^{-1}}$
g_{Na}	120	$\mathrm{ms\cdot cm^{-2}}$	d_2	1.049	$\mu\mathrm{mol\cdot L^{-1}}$
g_{K}	36	$\mathrm{ms\cdot cm^{-2}}$	d_3	0.9434	$\mu\mathrm{mol\cdot L^{-1}}$
E_{L}	−54.4	mV	d_5	0.08234	$\mu\mathrm{mol\cdot L^{-1}}$
E_{Na}	50	mV	a_2	0.2	$\mu\mathrm{mol\cdot L^{-1}\cdot s^{-1}}$
E_{K}	−77	mV	$[\mathrm{Ca^{2+}}]_{\mathrm{th}}$	0.2	$\mu\mathrm{mol\cdot L^{-1}}$
θ	2	–	V_{si}	−70	mV
δ	20	–	V_{se}	0	mV
k	0.5	$\mathrm{s^{-1}}$	α_s	0.1	$\mathrm{s^{-1}}$
$[\mathrm{IP_3}]^*$	0.16	$\mu\mathrm{mol\cdot L^{-1}}$	β_s	0.05	$\mathrm{s^{-1}}$
$1/\tau_{\mathrm{IP_3}}$	0.14	$\mathrm{s^{-1}}$	$\tau_{\mathrm{Ca^{2+}}}$	6	s
c_0	2.0	$\mu\mathrm{mol\cdot L^{-1}}$	g_{si}	0.6	$\mathrm{ms\cdot cm^{-2}}$
c_1	0.185	–	g_{se}	0.05	$\mathrm{ms\cdot cm^{-2}}$
v_1	6	$\mathrm{s^{-1}}$	ε_1	variable	–
v_2	0.11	$\mathrm{s^{-1}}$	ε_2	variable	–
v_3	0.9	$\mu\mathrm{mol\cdot L^{-1}}$	$r_{\mathrm{IP_3}}$	variable	$\mu\mathrm{M\cdot s^{-1}}$

A major goal of this paper is to study the temperature affecting the synchronization between pyramidal cells and interneurons under the regulation of astrocytes. For illustrative purposes, we use the maximum synchronization error[53] of the neuron membrane potential $\max(|e|)$ defined as

$$\max(|e|) = \max(|V_{\mathrm{IN}} - V_{\mathrm{PY}}|). \quad (14)$$

The maximum synchronization error $\max(|e|)$ can measure completely the synchronization in the oscillation of membrane potentials of pyramidal cells and interneurons. The lower the value of $\max(|e|)$, the stronger the neuron synchronicity, and the higher the value, the weaker the synchronicity.

Along with the order parameter $\max(|e|)$, we have also calculated a more common order parameter, the phase difference $\Delta\varphi$,[54,55]

$$\Delta\varphi = 2\pi\frac{t_{\mathrm{s}} - t_1}{t_2 - t_1}, \quad t_1 < t_{\mathrm{s}} < t_2, \quad (15)$$

where t_1 and t_2 are the corresponding times of the adjacent peak action potentials in the pyramidal cell. t_{s} is the time corresponding to the peak action potential of the interneuron. $\Delta\varphi$ is bounded between 0 and 2π. When the fixed phase difference

is not completely 0 or 2π,the neuron is in the out-of-phase synchronization state. For states with in-phase synchronization, $\Delta\varphi = 0$ or 2π. When the two neurons are in an asynchronous state, the phase difference presents a disordered state. In calculation, ordinary differential equations were solved using the Euler algorithm with a time step of 0.01 ms.

3. Results

3.1. Effect of r_{IP_3} on the electrical activity of thermosensitive neurons

First, we study the effect of IP_3 production rate on the discharge synchronization in thermosensitive neurons. Max($|e|$) was calculated between a pyramidal cell and an interneuron depending on the temperature T (0 °C $< T <$ 40 °C) for various rates of IP_3 production ($r_{IP_3} = 0$ μM·s^{-1}, 0.7 μM·s^{-1}, 1.7 μM·s^{-1}, 3 μM·s^{-1}) in Fig. 2.

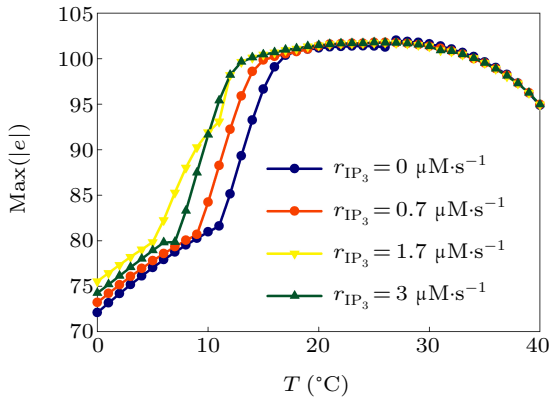


Fig. 2. Maximum synchronization error of neurons (max($|e|$)) with astrocytes depending on the temperature (T) for various IP_3 production rates (r_{IP_3}) ($\varepsilon_1 = 1$, $\varepsilon_2 = 1$, 0 °C $< T <$ 40 °C).

According to Fig. 2, the variation of max($|e|$) is related to temperature. Specifically, a range of temperature, approximately 18 °C $< T <$ 30 °C, is associated with the weak synchronization of two neurons. Max($|e|$) first increases and then later decreases with an increase in IP_3 production rate, which reaches the maximum at $r_{IP_3} = 1.7$ μM·s^{-1}. In the range 18 °C $< T <$ 40 °C, max($|e|$) does not show significant differences in the regulation of r_{IP_3}. It is shown that the increase in IP_3 production rate can induce a weak synchronization effect of neurons. In addition, at a range of temperatures, r_{IP_3} can induce weak synchronization.

In order to obtain more details about the effects of T and r_{IP_3} on the synchronization of two neurons, we calculate the maximum synchronization error max($|e|$) of two neurons in a wide range of T ($T = 0$ °C–40°C) and r_{IP_3} ($r_{IP_3} = 0$ μM·s^{-1}–3 μM·s^{-1}). The results are presented in T–r_{IP_3} parameter space in Fig. 3.

In Fig. 3, a certain region constraint by r_{IP_3} and T represents weak synchronization, and max($|e|$) reaches the maximum at about 23 °C. The trend of max($|e|$) is consistent with that reflected in Fig. 2. There is a triangular region of weak irregular variation with an increase of r_{IP_3} at 0 °C $< T <$ 37 °C. In this region, when r_{IP_3} increases to a certain threshold, the synchronization is not affected by r_{IP_3}. In addition, the threshold decreases with an increase in temperature. However, the trend of max($|e|$) increase is approximately linear above 37 °C. In other words, the higher the temperature, the harder it is to change the neuronal discharge synchronization under the regulation of astrocytes. It is indicated that increased temperature reduces the synchronization sensitivity of astrocytes about r_{IP_3}.

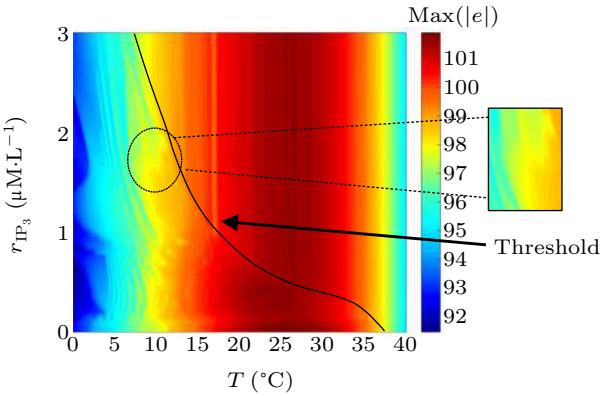


Fig. 3. Contour map of max($|e|$) depending on the IP_3 production rate (r_{IP_3}) and the temperature (T) ($\varepsilon_1 = 1$, $\varepsilon_2 = 1$, 0 °C $< T <$ 40 °C).

To quantify the phase synchronization of two neurons at a certain temperature, the phase difference ($\Delta\varphi$) as a function of IP_3 production rate is shown in Fig. 4. In Fig. 3, the different synchronization state features under different temperatures are obvious. In order to study the typical synchronization situation, we select the temperature values of 10 °C, 18 °C, and 23 °C to analyze the relationship between phase synchronization and the astrocyte parameters.

When $T = 10$ °C, the neurons are in an out-of-phase synchronization state, and the astrocytes have no effect on the phase synchronization of the neurons within the set parameter range in Figs. 4(a)–4(d). At $T = 18$ °C, when the feedback intensity of the astrocytes is sufficiently large, the phase of the neurons can shift from out-of-phase synchronization to an asynchronous state in Figs. 4(e)–4(h). For example, the neurons enter the asynchronous state when r_{IP_3} exceeds 0.7 in Fig. 4(h). At $T = 23$ °C, the neurons are under weak synchronization in Figs. 4(i)–4(l). When the feedback intensity of the astrocytes is small, the two neurons tend to stay in an out-of-phase synchronization state. Under this condition, r_{IP_3} does not change the phase synchronization state of the two neurons as the feedback intensity is too low to induce the asynchronous state. According to Figs. 4(j)–4(l), in the range of 0 μM·s^{-1} $< r_{IP_3} <$ 0.6 μM·s^{-1}, the phase of the neurons changes from out-of-phase synchronous to asynchronous with

an increase in r_{IP_3}. When r_{IP_3} increases to 0.6 $\mu M \cdot s^{-1}$, the two neurons are stable in an asynchronous state. It is shown that the variation in r_{IP_3} affects the phase synchronization at a temperature under weak synchronization.

In order to investigate the interaction mechanism between IP_3 concentration, Ca^{2+} concentration and neuronal synchronization, the time series of IP_3, Ca^{2+} concentration and two neuron membrane potentials are shown in Fig. 5.

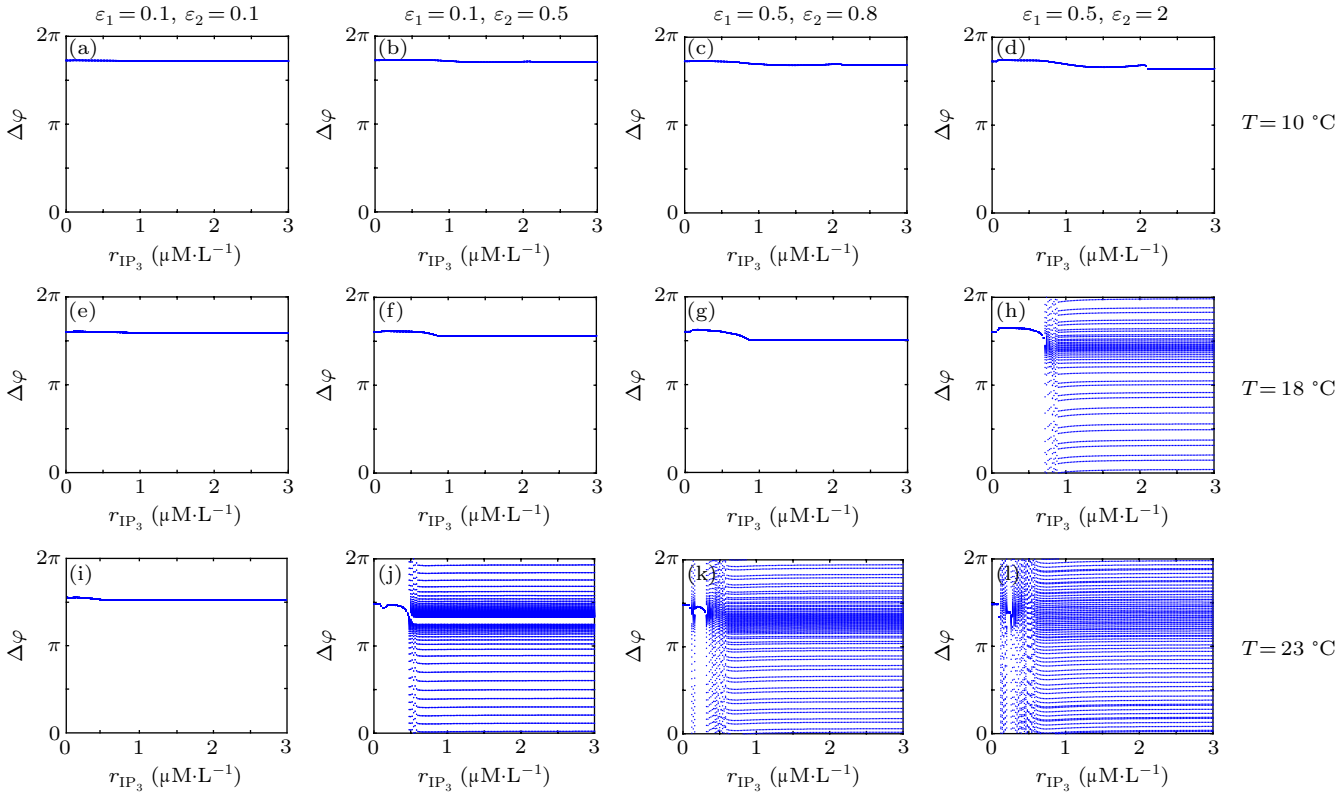


Fig. 4. Three row pictures represented by the phase difference with the action of different r_{IP_3} with $T = 10$ °C, $T = 18$ °C, and $T = 23$ °C from top to bottom.

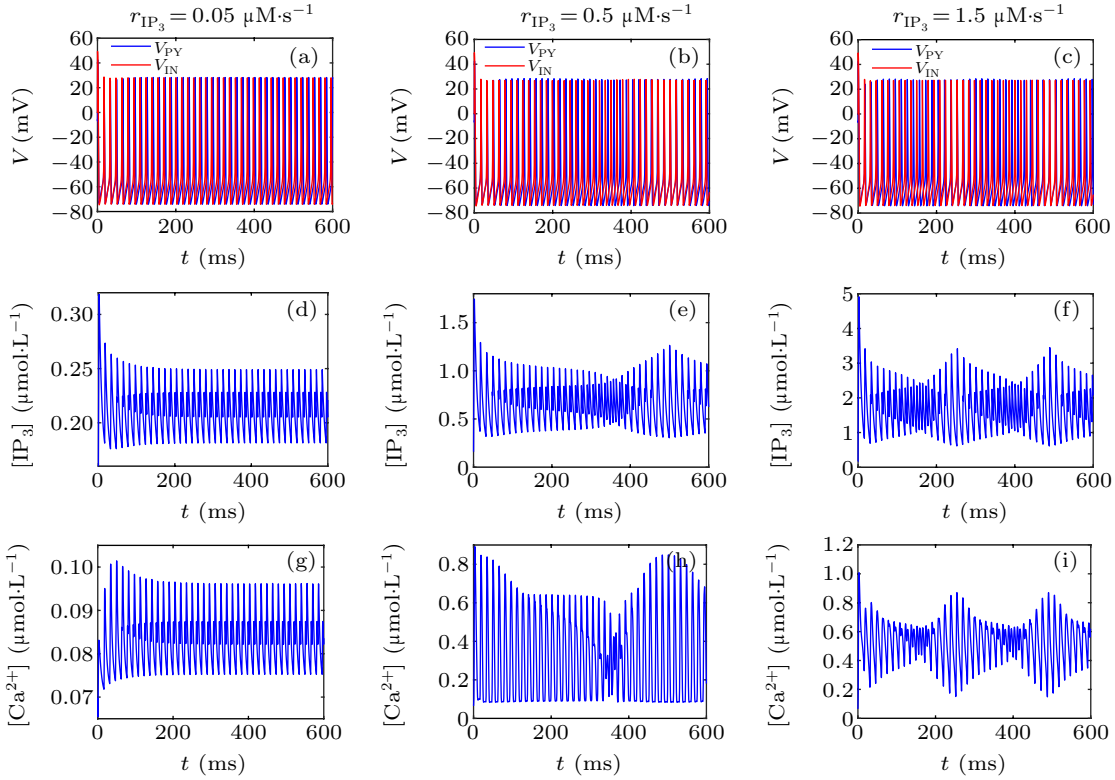


Fig. 5. Three rows of images representing the time series of neuronal membrane potential, IP_3 concentration and Ca^{2+} concentration from top to bottom. ($\varepsilon_1 = 0.5$, $\varepsilon_2 = 2$, $T = 23$ °C).

It is shown that the two neurons are in the state of peak firing with several values of r_{IP_3} at $T = 23$ °C under weak synchronization in Figs. 5(a)–5(c). The state of the neurons in Fig. 5(a) is out-of-phase synchronous. The state of the neurons in Figs. 5(b) and 5(c) is asynchronous, with another representation of the characteristics of intermittent synchronization. Comparing the results in Figs. 5(d) and 5(g), Figs. 5(e) and 5(h) to Figs. 5(f) and 5(i), respectively, the envelope curves of IP_3 and Ca^{2+} concentration oscillate. In addition, the oscillation frequency increases with an increase in r_{IP_3}. Thus, the high oscillation frequency of the envelope curves is accompanied by the asynchronous phenomenon of neurons. Moreover, at the peak of the envelope curves of IP_3 and Ca^{2+} concentration, the neuronal discharges are in synchronization. Therefore, the spiking synchronization is related to the peaks of the envelope curves of IP_3 and Ca^{2+} concentration.

3.2. Effect of ε_1 on the electrical activity of thermosensitive neurons

The ε_1 is one of the important coefficients of negative feedback in the communication between an astrocyte and a pyramidal cell. Indeed, the parameter ε_1 can reflect the inactivation intensity of ATP concentration produced by the astrocyte to the excitatory pyramidal cell.

For the purpose of investigating the role of the negative feedback coefficient of astrocytes on the synchronization of thermosensitive neurons, we calculate max($|e|$) with different values of ε_1 ($\varepsilon_1 = 0, 1, 2, 3$) in the temperature range 0 °C $< T <$ 40 °C. The comparison curve for different values of ε_1 is shown in Fig. 6.

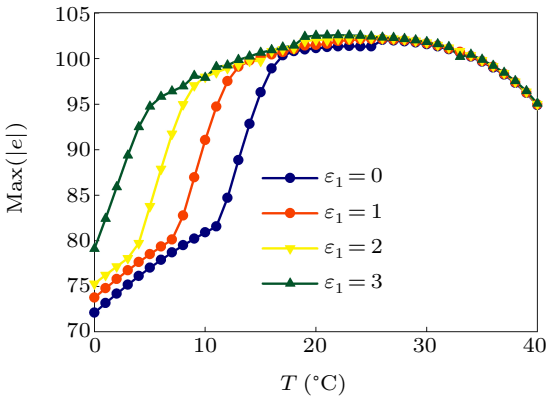


Fig. 6. Maximum synchronization error of neurons (max($|e|$)) with astrocytes depending on the temperature (T) for various negative feedback coefficients (ε_1) ($r_{IP_3} = 0.8\ \mu M \cdot s^{-1}$, $\varepsilon_2 = 0.1$, 0 °C $< T <$ 40 °C).

As shown in Fig. 6, with an increase in temperature, max($|e|$) first rises sharply and then decreases. When the temperature is varied over the range 0 °C–18 °C, max($|e|$) increases with an increase in ε_1. This trend of max($|e|$) means that the increase in the negative feedback coefficient plays a role in the weak synchronization of neurons. In addition, when 27 °C $< T <$ 40 °C, max($|e|$) hardly changes with an increase in ε_1. Accordingly, the negative feedback coefficient and temperature have a great influence on the synchronization of neurons. Moreover, when the negative feedback coefficient $\varepsilon_1 = 3$, weak synchronization occurs in the temperature range 19 °C $< T <$ 26 °C.

To investigate the phenomenon in more detail, we calculate the maximum synchronization error max($|e|$) in a wide range of negative feedback coefficient ε_1 ($\varepsilon_1 = 0$–3) and temperature T ($T = 0$ °C–40 °C). The obtained results are presented in T–ε_1 parameter space in Fig. 7.

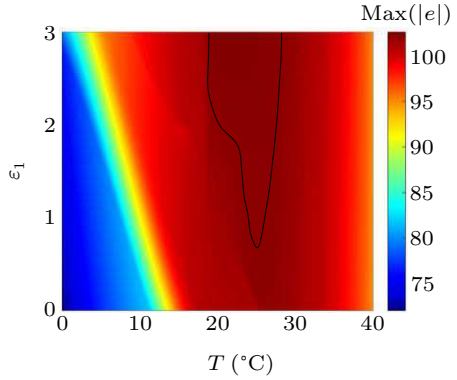


Fig. 7. Contour plot of max($|e|$) depending on negative feedback coefficient (ε_1) of astrocytes to pyramidal cells and temperature (T) ($r_{IP_3} = 0.8\ \mu M \cdot s^{-1}$, $\varepsilon_2 = 0.1$, 0 °C $< T <$ 40 °C).

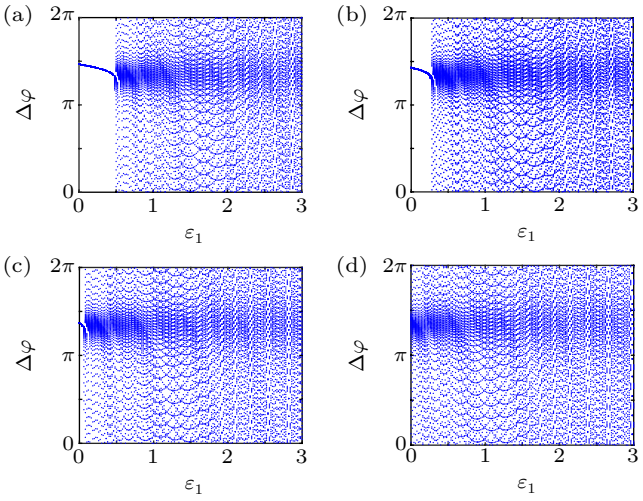


Fig. 8. Phase difference with the action of different ε_1 with (a) $r_{IP_3} = 0.8\ \mu M \cdot s^{-1}$, $\varepsilon_2 = 0.1$, (b) $r_{IP_3} = 0.8\ \mu M \cdot s^{-1}$, $\varepsilon_2 = 0.3$, (c) $r_{IP_3} = 0.8\ \mu M \cdot s^{-1}$, $\varepsilon_2 = 0.5$, (d) $r_{IP_3} = 0.8\ \mu M \cdot s^{-1}$, $\varepsilon_2 = 0.7$ ($T = 23$ °C).

It is obvious that the oscillation behavior of neurons appears with the change in temperature and feedback coefficient for max($|e|$) intuitively shown in Fig. 7. The maximal region of max($|e|$) (red irregular area in Fig. 7) results from a range of T and ε_1, which are selected at 19 °C $< T <$ 28 °C, $0.7 < \varepsilon_1 < 3$. The maximal region of max($|e|$) represents weak synchronization, which is consistent with the temperature range and negative feedback intensity value in Fig. 6. Interestingly, we find that the value of max($|e|$) presents an obvious segmentation line in the combination range of T and ε_1 (0 °C $< T <$ 16 °C, $0 < \varepsilon_1 < 3$). The area on the left of the

segmentation line is in stronger synchronization, and that on the right is in weaker synchronization.

In addition, for temperature ($T = 23$ °C) under weak synchronization, the phase synchronization of neurons with changing negative feedback coefficient ($0 < \varepsilon_1 < 3$) is shown in Fig. 8.

As shown in Fig. 8(a), when $\varepsilon_2 = 0.1$, the two neurons are in a state of out-of-phase synchronization, and the phase differences are between 0 and 2π. As ε_1 exceeds 0.5, the phase differences become chaotic, and their values are irregular between 0 and 2π. In this state, the two neurons fire asynchronously. In Fig. 8(b), when $\varepsilon_2 = 0.3$, the two neurons are in a state of out-of-phase synchronization. As ε_1 exceeds 0.25, the phase differences become chaotic, and the two neurons become asynchronous. In Figs. 8(c) and 8(d), the neurons remain almost asynchronous with a change in ε_1. Thus, the synchronous state of the neurons transits from out-of-phase synchronization to asynchronous with an increase in ε_1. Through comparison of Figs. 8(a)–8(d), it can be seen that the threshold of ε_1 for the neuron transition to the asynchronous state decreases gradually with an increase in ε_2. Significantly, the negative feedback overactivation of astrocytes to neurons leads to an asynchronous state in the neuron–astrocyte system. It is speculated that the increase in negative feedback intensity may promote confusion of pyramidal cell discharge and the asynchronous state of neurons.

In some cases, the Ca^{2+} concentration is possibly associated with the two neurons' synchronization. To investigate the relationship between the synchronization and the concentration changes of IP_3 and Ca^{2+}, figure 9 depicts the time series of IP_3, Ca^{2+} concentration and the two neurons' membrane potentials under various ε_1 ($\varepsilon_1 = 0.3, 1.3, 2.3$).

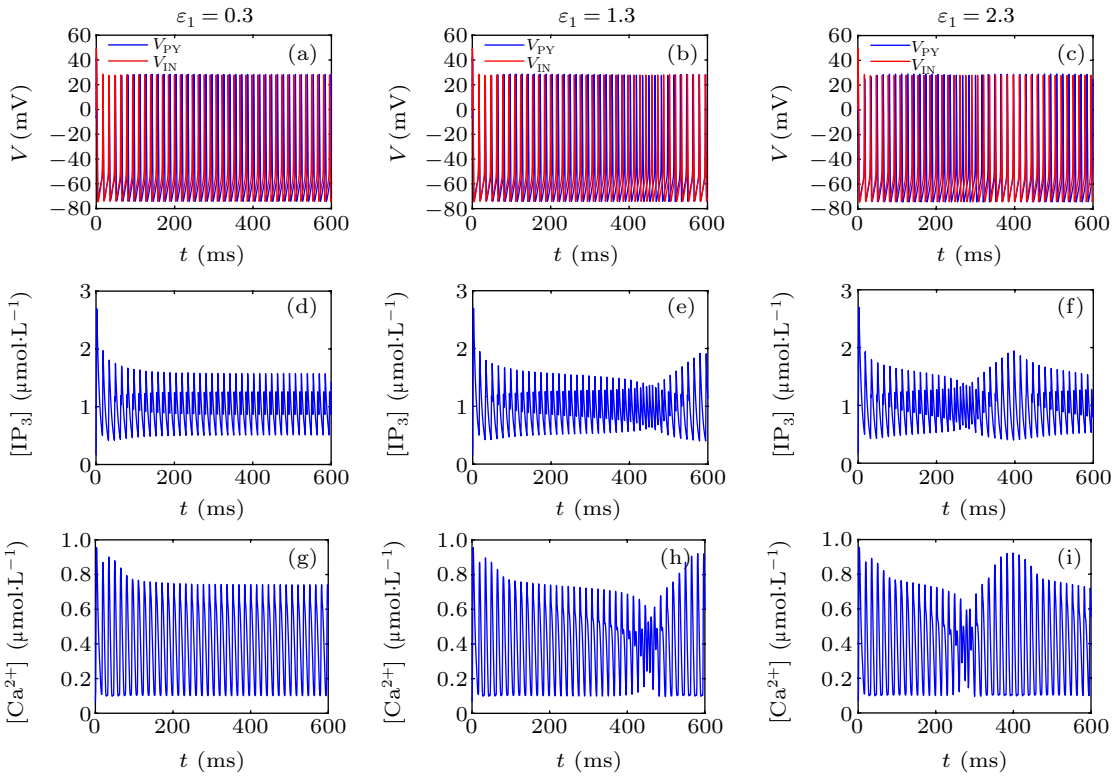


Fig. 9. Three rows of images representing the time series of neuronal membrane potential, IP_3 and Ca^{2+} concentration from top to bottom ($r_{IP_3} = 0.8\ \mu M \cdot s^{-1}$, $\varepsilon_2 = 0.1$) ($T = 23$ °C).

In order to study the dynamic mechanism of the effects of IP_3 and Ca^{2+} concentration on the neuronal membrane potential, we take the temperature under weak synchronization ($T = 23$ °C). It is shown that the two neurons are in the state of peak firing under weak synchronization in Figs. 9(a)–9(c). Specifically, figure 9(a) illustrates the out-of-phase synchronous state, and figures 9(b) and 9(c) illustrate the asynchronous state. Meanwhile, the wave crest spacing of envelope curves of IP_3 and Ca^{2+} concentration decreases gradually with an increase in ε_1. In other words, with an increase in ε_1, the oscillation frequency of the IP_3 and Ca^{2+} concentration envelope curves increases. The above analysis clearly shows that the asynchronous phenomenon of neurons is related to the high-frequency oscillation of the IP_3 and Ca^{2+} concentration envelope curves.

3.3. Effect of ε_2 on the electrical activity of thermosensitive neurons

Finally, the parameter ε_2 can reflect the activation intensity of the glutamate concentration produced by astrocytes to inhibitory interneurons. We discuss the effect of a positive feedback coefficient of an astrocyte on the maximum synchro-

nization error in the neuron–astrocyte minimum system. The curves of max($|e|$) depending on T are shown in Fig. 10 for different feedback coefficients ($\varepsilon_2 = 0, 1, 2, 3$).

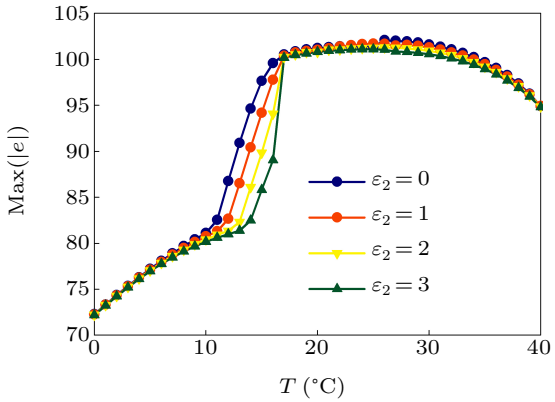


Fig. 10. Maximum synchronization error of neurons (max($|e|$)) with astrocytes depending on the temperature (T) for various positive feedback coefficients (ε_2) ($r_{IP_3} = 0.8\ \mu M \cdot s^{-1}$, $\varepsilon_1 = 0.1$, $0\ ^\circ C < T < 40\ ^\circ C$).

According to Fig. 10, the maximum synchronization error max($|e|$) first increases with T and then decreases after exceeding 26 °C. When the temperature is below 18 °C, the curves of max($|e|$) slightly decrease as ε_2 increases. This means that the increase in ε_2 promotes the synchronization level of neurons. The results of Fig. 10 show the opposite characteristics to ε_1 (Fig. 6). This discrepancy may be due to the different feedback characteristics of astrocytes to pyramidal cells and interneurons.

In order to obtain detailed information on the synchronization of neurons affected by the variation in both ε_2 and T, we select a wide range of ε_2 ($0 < \varepsilon_2 < 3$) and T ($0\ ^\circ C < T < 40\ ^\circ C$) to calculate the maximum synchronization error max($|e|$) of neurons in Fig. 11.

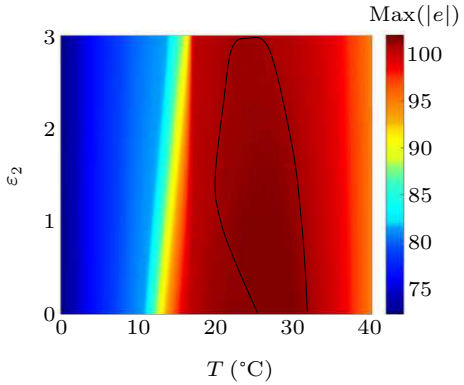


Fig. 11. Contour plot of max($|e|$) depending on positive feedback coefficient (ε_2) of astrocytes to interneurons and temperature (T) ($r_{IP_3} = 0.8\ \mu M \cdot s^{-1}$, $\varepsilon_1 = 0.1$, $0\ ^\circ C < T < 40\ ^\circ C$).

In Fig. 11, the region in red represents almost weak synchronization of neurons, which is probably the maximal value of max($|e|$) in the range of ε_2 ($0 < \varepsilon_2 < 3$, $20\ ^\circ C < T < 32\ ^\circ C$). The results mean the interaction between astrocytes and thermosensitive neurons depends on ε_2 and T under weak synchronization, which echoes the verification of Fig. 10. Similar to ε_1, under the joint action of ε_2 and T, there is also a line dividing areas of synchronization level. The area on the left of the line is with a stronger synchronization level, and that on the right is with a weaker synchronization level. It is interpreted that the synchronization of neurons can be changed by adjusting to a suitable feedback coefficient of astrocytes. In addition, compared with the negative feedback of astrocytes in Fig. 7, the positive feedback effect is weaker in regulatory synchronization.

Figure 12 depicts the change in phase synchronization of neurons under the influence of ε_2 ($0 < \varepsilon_2 < 3$) at temperature ($T = 23\ ^\circ C$) under weak synchronization.

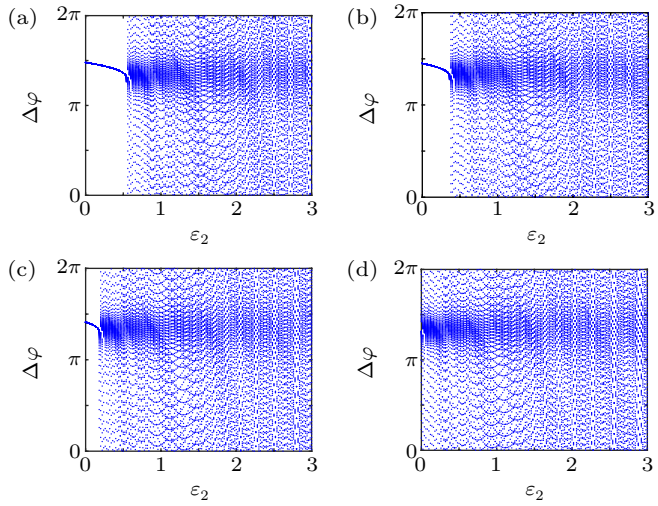


Fig. 12. Phase difference with the action of different ε_2 with (a) $r_{IP_3} = 0.8\ \mu M \cdot s^{-1}$, $\varepsilon_1 = 0.01$, (b) $r_{IP_3} = 0.8\ \mu M \cdot s^{-1}$, $\varepsilon_1 = 0.2$, (c) $r_{IP_3} = 0.8\ \mu M \cdot s^{-1}$, $\varepsilon_1 = 0.4$, (d) $r_{IP_3} = 0.8\ \mu M \cdot s^{-1}$, $\varepsilon_1 = 0.6$ ($T = 23\ ^\circ C$).

As shown in Fig. 12(a), when $\varepsilon_1 = 0.01$, the two neurons are in a state of out-of-phase synchronization in the range of $0 < \varepsilon_2 < 0.55$, and the phase differences are between 0 and 2π. As ε_2 exceeds 0.55, the phase differences become chaotic, and their values are irregular between 0 and 2π. In this state, the two neurons fire asynchronously. When $\varepsilon_1 = 0.2$, the two neurons are in a state of out-of-phase synchronization in the range $0 < \varepsilon_2 < 0.4$ in Fig. 12(b). As ε_2 exceeds 0.4, the phase differences become chaotic, and the two neurons become asynchronous. Similarly, when $\varepsilon_1 = 0.4$ and ε_2 exceeds 0.2, the two neurons transit from out-of-phase synchronization to asynchronization in Fig. 12(c). When $\varepsilon_1 = 0.6$, ε_2 can only cause the asynchronous phenomenon of neurons as shown in Fig. 12(d). As with the regulation of ε_1, the phase synchronization of two neurons transits from the out-of-phase synchronization to the asynchronous state when the strength of positive feedback (ε_2) reaches a certain threshold. According to Figs. 12(a)–12(d), an increase in ε_1 promotes the critical value of the neuron synchronization state transition to become smaller. It is indicated that the negative feedback of astrocytes to excitatory pyramidal cells and the positive feedback

to inhibitory interneurons have the same effect on the phase transition between neurons.

In order to further investigate the effect on network synchronization development by gliotransmitter diffusion, we discuss the relations between the concentrations of IP_3 and Ca^{2+} and synchronization with various ε_2 ($\varepsilon_2 = 0.5, 1.5, 2.5$) at the temperature of weak synchronization ($T = 23$ °C) in Fig. 13.

Figures 13(a)–13(c) show the membrane potential of two neurons, which are in a state of peak firing. At $\varepsilon_2 = 0.5$, the neurons are in an out-of-phase synchronous state in Fig. 13(a). At $\varepsilon_2 = 1.5$ in Fig. 13(b) and $\varepsilon_2 = 2.5$ in Fig. 13(c), the neurons are in an asynchronous state. Compared with Figs. 13(d)–13(f), the peak-to-peak spacing of the IP_3 concentration envelope curves gradually decreases. Likewise, compared with Figs. 13(g)–13(i), the peak-to-peak spacing of the Ca^{2+} concentration envelope curves decreases. Moreover, the envelope curve peaks of IP_3 and Ca^{2+} concentration correspond to the spiking synchronization of neuronal membrane potential. The results are the same as the characteristics of ε_1.

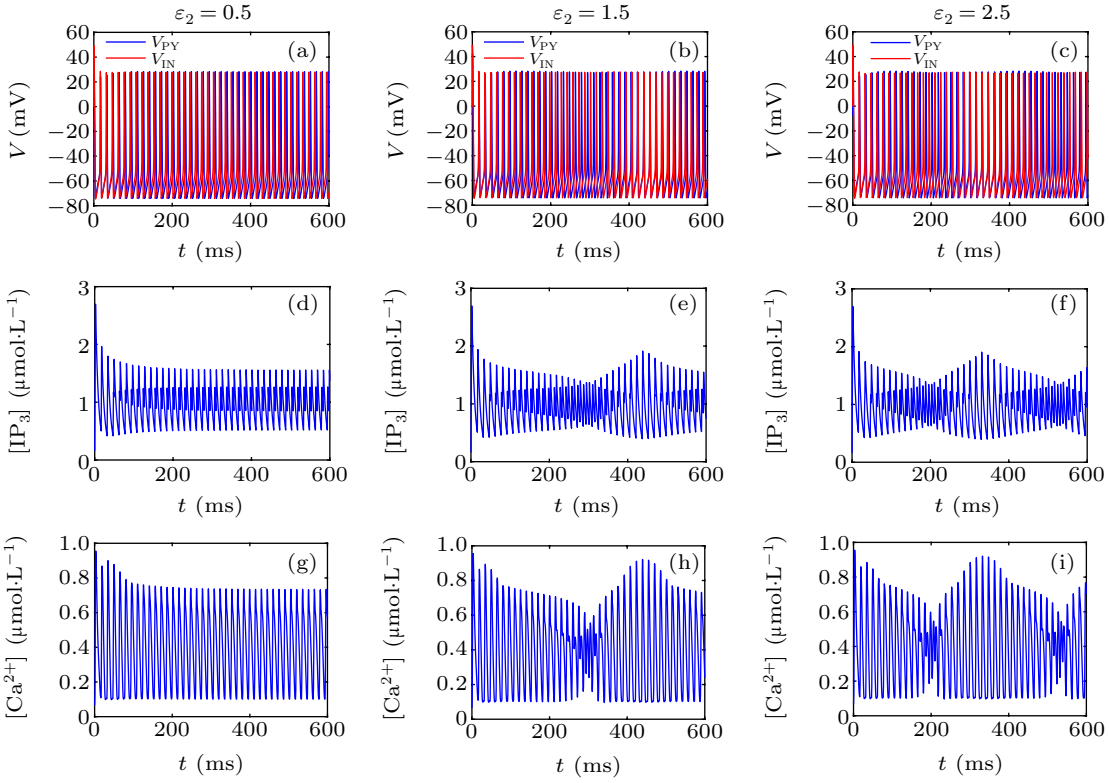


Fig. 13. Three rows of images representing the time series of neuronal membrane potential, IP_3 and Ca^{2+} concentration from top to bottom. ($r_{IP_3} = 0.8$ μM·s^{-1}, $\varepsilon_1 = 0.01$) ($T = 23$ °C).

4. Discussion and conclusion

It has been widely verified that temperature plays an important role in neuronal discharge and astrocyte function by many experiments. Hence, we studied and analyzed the dynamic mechanism of a temperature-dependent neuron–astrocyte coupling system in this paper. We focused on the synchronization in the thermosensitive neuron–astrocyte minimum system.

Firstly, it is indicated that the synchronization of neurons under the influence of temperature can be nonlinearly regulated by the IP_3 production rate in astrocytes and the feedback coefficients of astrocytes to pyramidal cells and interneurons. Recently, experiments have shown that the apoptosis and activation of astrocytes are inhibited by low temperature.[40] In this paper, we also observed that neuronal synchronization was strongly regulated by the presence of astrocytes at low temperature (probably 0 °C $< T <$ 18 °C). This phenomenon probably results from astrocytes which are not fully activated under the condition of low temperature. Additionally, the change of temperature can lead to a change in the activation degree of astrocytes. Therefore, under the condition of low temperature, astrocytes have a stronger synchronous regulation effect on neurons. However, it is a little effect that the astrocytes impose on the synchronization between pyramidal cells and interneurons in the normal physiological temperature range of the brain. It is shown that astrocytes are more likely to be fully activated with increased temperature, interacting with neurons to stabilize the brain. Note that this is consistent with some results of previous experiments.[40,41] More interestingly, the experiment in Ref. [56] showed that an increase in temperature leads to a decrease in the behavior variability of single neurons. In this paper, it is further verified that the influence

of astrocytes on the behavioral variability of neurons decreases with increasing temperature.

In addition, it is revealed that the synchronization between pyramidal cells and interneurons can be prominently decreased by the temperature at a range of IP_3 production rates ($0.2\ \mu M\cdot s^{-1} < r_{IP_3} < 3\ \mu M\cdot s^{-1}$). For feedback coefficients of astrocytes, the maximum synchronization error of neurons exhibits a similar dependence on the negative and positive feedback intensities of astrocytes to neurons. It is shown that corresponding temperature and feedback coefficients can promote the state of weak synchronization of neurons. In particular, comparing the effects of ε_1 (Figs. 6 and 7) and ε_2 (Figs. 10 and 11) on the synchronization of two neurons, it is indicated that the change of neuronal synchronization is more dependent on the negative feedback intensity of astrocytes to pyramidal cells. In other words, the regulation of astrocytes on pyramidal cells is more efficient than that on interneurons, even with the same feedback coefficients.

Then, we studied the effect of a change in IP_3 production rate and the feedback coefficients of astrocytes on the phase synchronization of two neurons at temperature ($T = 23\ ^\circ C$). The two neurons can be in weak synchronization at 23 °C. According to the phase diagrams of Figs. 4, 8 and 12, with an increase of IP_3 production rate and feedback intensities for astrocytes, two neurons transit from out-of-phase synchronization to an asynchronous state at the temperature of weak synchronization.

Finally, we studied the interaction mechanism between synchronization and the concentrations of IP_3 and Ca^{2+} at a temperature under weak synchronization ($T = 23\ ^\circ C$). With increases in r_{IP_3}, ε_1, and ε_2, the oscillation frequency of the IP_3 and Ca^{2+} concentration envelope curves increases, and the peak-to-peak distance of the envelope curves decreases. Note that we have previously analyzed that an increase in astrocyte parameters promoted the phase transition of neurons. The phase transition of neurons is closely related to the oscillation frequency and peak-to-peak distance of the envelope curves of IP_3 and Ca^{2+} concentration. Furthermore, we found that intermittent synchronization occurs when neurons are in an asynchronous state. This result is consistent with the finding that astrocytes can induce intermittent synchronization of neurons in Ref. [26]. In particular, Makovkin[26] showed that the frequency of calcium oscillations in astrocytes was not sensitive to the synchronization between neurons. However, we found that the frequency of the Ca^{2+} concentration envelope was related to the phase synchronization of neurons. Analyzing the results of the neuronal membrane potential and the Ca^{2+} concentration, it was observed that the envelope curve peaks of Ca^{2+} concentration corresponded to the spiking synchronization state of neurons. This difference in results may be due to the temperature fact. In summary, it is interpreted that the neuronal discharge activity is regulated by Ca^{2+}, a result that is consistent with Ref. [50].

When the synchronization level of neurons is very weak, cognitive function is impeded. In this paper, we have studied a synchronous regulation mechanism based on a thermosensitive neuron–astrocyte minimum system model in the hippocampus, especially under the temperature of weak synchronization. These results can provide a helpful basis to understanding cognitive impairment and treating nervous system diseases. In future work, we will consider a complex model more approximate to a realistic brain, including more functional neurons, e.g., dopaminergic neurons, medial septum neurons and guardian neurons in the preoptic area of the hypothalamus. We hope to contribute to the exploration of the mechanism of cognitive dysfunction and neurological disorders such as epilepsy.

Acknowledgments

Project supported by the National Natural Science Foundation of China (Grant Nos. 51607056, 51737003, and 51877069) and State Key Laboratory of Reliability and Intelligence of Electrical Equipment, Hebei University of Technology (Grant No. EERI_PI2020006).

References

[1] Shu R, Chen W and Xiao J H 2019 *Acta Phys. Sin.* **68** 180503 (in Chinese)
[2] Ding X L, Jia B and Li Y Y 2019 *Acta Phys. Sin.* **68** 180502 (in Chinese)
[3] Han F, Wang Z J, Fan H and Gong T 2015 *Chin. Phys. Lett.* **32** 040502 (in Chinese)
[4] Duan L, Liu C, Zhao L C and Yang Z Y 2020 *Acta Phys. Sin.* **69** 010501 (in Chinese)
[5] Zhang D, Shi J Q, Sun Y, Yang X H and Ye L 2019 *Acta Phys. Sin.* **68** 240502 (in Chinese)
[6] Wang T, Zhou M Y and Fu Z Q 2020 *Chin. Phys. B* **29** 058901
[7] Yue X L, Xiang Y L and Zhang Y 2019 *Acta Phys. Sin.* **68** 180501 (in Chinese)
[8] Shao S L, Wang T, Song C H, Cui E N, Zhao H and Yao C 2019 *Acta Phys. Sin.* **68** 178701 (in Chinese)
[9] Zhao W L and Jie Q L 2020 *Chin. Phys. B* **29** 080302
[10] Ouannas A, Khennaoui A A, Momani S, Pham V T and Khazali R E 2020 *Chin. Phys. B* **29** 050504
[11] Chen C, Ding Z X, Li S and Wang L H 2020 *Chin. Phys. B* **29** 040202
[12] Li J H 2016 *Chin. Phys. Lett.* **33** 120501
[13] Sun J C 2016 *Chin. Phys. Lett.* **33** 100503
[14] Wang R, Guo J B, Hui J P, Wang Z, Liu H J, Xu Y N and Liu Y F 2019 *Acta Phys. Sin.* **68** 180701 (in Chinese)
[15] Ding P F, Feng X Y and Wu C M 2020 *Chin. Phys. B* **29** 108202
[16] Huang F, Chen H S and Shen C S 2015 *Chin. Phys. Lett.* **32** 118902
[17] Wang Y X, Zhai J Q, Xu W W, Sun G Z and Wu P H 2015 *Chin. Phys. Lett.* **32** 097401
[18] Zhai J Q, Li Y C, Shi J X, Zhou Y, Li X H, Xu W W, Sun G Z and Wu P H 2015 *Chin. Phys. Lett.* **32** 047402
[19] Huang J W, Lv S X, Zhang Z S and Yuan H Q 2020 *Chin. Phys. B* **29** 060505
[20] Araque A, Parpura V, Sanzgiri R P and Haydon P G 1999 *Trends Neurosci.* **22** 208
[21] Du M M, Li J J, Yuan Z X, Fan Y C and Wu Y 2020 *Chin. Phys. B* **29** 038701
[22] Amiri M, Montaseri G and Bahrami F 2011 *Biol. Cybern.* **105** 153
[23] Araque A, Carmignoto G, Haydon P G, Oliet S H R, Robitaille R and Volterra A 2014 *Neuron* **81** 728

[24] Porter J T and McCarthy D K D 1995 *Glia* **13** 101
[25] Nadkarni S and Jung P 2004 *Phys. Biol.* **1** 35
[26] Makovkin S Y, Shkerin I V, Gordleeva S Y and Ivanchenko M V 2020 *Chaos Soliton. Fract.* **138** 109951
[27] Ji Q B, Zhou Y, Yang Z Q and Meng X Y 2015 *Chin. Phys. Lett.* **32** 050501
[28] Nadkarni S and Jung P 2007 *Phys. Biol.* **4** 1
[29] Erkan Y, Saraç Z and Yılmaz E 2019 *Nonlinear Dyn.* **95** 3411
[30] Øyehaug L, Østby I, Lloyd C M, Omholt S W and Einevoll G T 2012 *J. Comput. Neurosci.* **32** 147
[31] Carmen D V, Sverre M S, Ecem A, Evelien V H, Celine D, Slike V, Julie V, Robbrecht P, Mehmet I C, Akira M, Caghan K, Koichi K, Nathalie J Y and Emre Y 2019 *Nat. Commun.* **10** 3830
[32] Kim J A and Connors B W 2012 *Front. Cell. Neurosci.* **6** 27
[33] Feudel U, Neiman A, Pei X, Wojtenek W, Braun H, Huber M and Moss F 2000 *Chaos* **10** 231
[34] Rossi K L, Budzinski R C, Boaretto B R R, Prado T L, Feudel U and Lopes S R 2021 *Chaos* **31** 083121
[35] Budzinski R C, Boaretto B R R, Prado T L and Lopes S R 2019 *Chaos Soliton. Fract.* **123** 35
[36] Xu Y, Liu M H, Zhu Z G and Ma J 2020 *Chin. Phys. B* **29** 098704
[37] DeMaegd M L and Stein W 2020 *PLoS Comput. Biol.* **16** e1008057
[38] Lu L L, Kirunda J B, Xu Y, Kang W J, Ye R, Zhan X and Jia Y 2018 *Eur. Phys. J. Special Top.* **227** 767
[39] Hyun N G, Hyun K, Oh S and Lee K 2020 *Korean J. Physiol. Pharmacol.* **24** 349
[40] Kitamura M, Ishikawa K, Nei K, Nakajima K, Yamanoha B and Shimizu A 2018 *High Pressure Res.* **38** 348
[41] Leisengang S, Ott D, Gerstberger R, Rummel C and Roth J 2018 *Neuroreport* **29** 1468
[42] Zhang Y H, Liu H, Han Y R, Chen Y F, Zhang S H and Zhan Y 2017 *Chin. Phys. Lett.* **34** 098701
[43] Du M M, Li J J, Wu Y and Yu G Y 2021 *Cogn. Neurodyn.*
[44] Hodgkin A L and Huxley A F 1990 *Bull. Math. Biol.* **52** 25
[45] Fujisaki T, Wakatsuki H, Kudoh M and Shibuki K 1999 *Neurosci. Res.* **33** 307
[46] Postlethwaite M, Hennig M H, Steinert J R, Graham B P and Forsythe I D 2007 *J. Physiol.* **579** 69
[47] Braun H A, Huber M T, Dewald M, Schafer K and Voigt K 1998 *Int. J. Bifurcat. Chaos* **8** 881
[48] Hodgkin A L and Huxley A F 1952 *J. Physiol.* **117** 500
[49] Tchaptchet A 2018 *Chaos* **28** 106327
[50] Yu Y Y, Yuan Z X, Fan Y C, Li J J and Wu Y 2020 *Neural Plast.* **2020** 8864246
[51] Amiri M, Bahrami F and Janahmadi M 2012 *J. Theor. Biol.* **292** 60
[52] Li J J, Du M M and Wang R 2016 *Int. J. Bifurcat. Chaos* **26** 1650138
[53] Wang Q Y, Shi X and Lu Q C 2008 *Coupling System Synchronized Dynamics* (Beijing: Science Press) p. 62 (in Chinese)
[54] Budzinski R C, Boaretto B R R, Prado T L and Lopes S R 2019 *Commun. Nonlinear Sci.* **75** 140
[55] Wang J, Ye W J, Liu S Q, Liu B and Jiang X F 2016 *Chaos Soliton. Fract.* **93** 32
[56] Boaretto B R R, Budzinski R C, Prado T L, Kurths J and Lopes S R 2018 *Chaos* **28** 106304